

DEEP COUNTS OF SUBMILLIMETER GALAXIES

A. W. BLAIN,^{1,2} J.-P. KNEIB,² R. J. IVISON³ & IAN SMAIL⁴

1) Cavendish Laboratory, Madingley Road, Cambridge CB3 0HE, UK

2) Observatoire Midi-Pyrénées, CNRS-UMR5572, 14 Avenue E. Belin, 31400 Toulouse, France

3) Department of Physics & Astronomy, University College London, Gower Street, London, WC1E 6BT, UK.

4) Department of Physics, University of Durham, South Road, Durham DH1 3LE, UK

Received 1998 – –; accepted: 1998 – –

ABSTRACT

We present the counts of luminous submillimeter (sub-mm) galaxies from an analysis of our completed survey of the distant Universe seen through lensing clusters. This survey uses massive clusters lenses with well-constrained mass models to obtain a magnified view of the background sky. This both increases the sensitivity of our sub-mm maps and reduces the effects of source confusion. Accurate lens models are used to correct the observed sub-mm source counts for the lens amplification. We show that the uncertainties associated with this correction do not dominate the final errors. We present sub-mm counts derived from two independent methods: a direct inversion of the observed sources, which are corrected individually for lens amplification; and a Monte-Carlo simulation of our observations using a parametric model for the background counts, which is folded through the lens models and incompleteness estimates to determine best-fitting values of the count parameters. Both methods agree well and confirm the robustness of our analysis. Detections that are identified with galaxies in the lensing clusters in deep optical images (Smail et al. 1998) are removed prior to our analysis, and the results are insensitive both to the details of the correction and to the redshift distribution of the detections. We present the 850- μ m counts at flux densities between 0.5 and 8 mJy. The count of galaxies brighter than 4 mJy is $1500 \pm 700 \text{ deg}^{-2}$, in agreement with the value of $2500 \pm 1400 \text{ deg}^{-2}$ reported by Smail, Ivison & Blain (1997). The most accurate 850- μ m count is determined at 1 mJy: $7900 \pm 3000 \text{ deg}^{-2}$. All quoted errors include both Poisson and systematic terms. These are the deepest sub-mm counts published, and are not subject to source confusion because the detected galaxies are separated and magnified by the lens. Down to the 0.5-mJy limit of our counts, the resolved 850- μ m background radiation intensity is $(5 \pm 2) \times 10^{-10} \text{ W m}^{-2} \text{ sr}^{-1}$, comparable to the current *COBE* estimate of the background. This indicates that the bulk of the 850- μ m background radiation originated in distant ultraluminous galaxies.

Subject headings: cosmology: observations — gravitational lensing — galaxies: evolution — galaxies: formation — infrared: galaxies

1. INTRODUCTION

The Submillimetre Common-User Bolometer Array (SCUBA; Holland et al. 1999) on the James Clerk Maxwell Telescope (JCMT) has recently been used to detect a new population of extremely luminous distant dusty galaxies (Smail, Ivison & Blain 1997). By exploiting the strong magnification bias due to lensing through rich clusters of galaxies, we reach fainter detection thresholds in a given observing time, while suffering little contamination from cluster galaxies (Blain 1997). Consistent numbers of sources have also been detected in the field (Barger et al. 1998; Eales et al. 1998; Holland et al. 1998; Hughes et al. 1998). The results from these studies have important consequences for the history of star formation (Blain et al. 1999), and may also provide substantial insight into the prevalence of dust-enshrouded active galactic nuclei during the early evolution of galaxies (Ivison et al. 1998). Smail et al. (1997) estimated counts from six galaxies detected in maps of two clusters – A 370 and Cl2244–02 – using simple models of the clusters as singular isothermal spheres. The complete SCUBA lens survey sample includes deeper maps of these two clusters, and a further five clusters mapped to a sensitivity better than 2 mJy (Smail et al. 1998). The analysis of the maps and the

source extraction procedures are discussed by Smail et al. (1997). The full catalog of the SCUBA and follow-up data can be found elsewhere (Smail et al. in preparation). In this new self-contained analysis of the whole lens survey sample, we exploit models of the cluster potentials derived from deep *Hubble Space Telescope* (*HST*) and high-resolution ground-based optical imaging, and the LENSTOOL ray-tracing code (Kneib et al. 1993) to correct for the effects of lens amplification and calculate robust number counts of faint sub-mm galaxies below the flux limit of previously published work. The calculations are carried out in an Einstein–de Sitter world model, but the results depend only weakly on the world model assumed.

2. GALAXY COUNTS

In a blank field the cumulative sub-mm galaxy counts – the surface density of galaxies brighter than a given flux density limit – can be derived by simply dividing the number of detected sources by the surveyed area, although the effects of clustering may have to be considered in small fields. The calculation is more complicated in the field of a gravitational lens, which magnifies and distorts the background sky – the source plane – by an amount that depends on both position and redshift. As a result of lensing,

some regions of the source plane are observed to greater depths than others, even if the sensitivity across the observed map – the image plane – is uniform. With a sufficiently detailed mass model for the lens, corrections can be applied to model the effects of lensing accurately, and thus the enhanced sensitivity to faint background sources can be exploited. Moreover, lensing provides a further advantage: because sub-mm-wave telescopes have coarse angular resolution as compared with optical telescopes, source confusion can contribute noise in faint images (Blain, Ivison & Smail 1998; Hughes et al. 1998). The flux density of all background sources is increased by a lensing cluster, while their mean separation on the sky is also increased. Both of these features reduce the problem of confusion.

The lensing effect of the rich clusters exploited in the survey is modeled accurately by using multiple-component mass distributions that describe the extended potential well of the clusters and their more massive individual member galaxies (e.g. Kneib et al. 1996). These models are derived using the positions of multiply-imaged features identified in high-resolution optical images, and are very well constrained using the spectroscopic redshifts of these multiple images. Details of the mass models employed can be found in: C10024+16 (Smail et al. 1996); A 370 (Kneib et al. 1993; Bézecourt et al. 1999); MS 0440+02 (Gioia et al. 1998); C10939+47 (Seitz et al. 1996); A 1835 (Edge et al. 1999); A 2390 (Kneib et al. 1999); C12244–02 (Kneib private communication). The uncertainties in the magnification of background galaxies derived from these models are 10–20%, and so are comparable with the uncertainty in the absolute calibration of the SCUBA maps.

The lens amplification depends on both the redshift of the lens (z_l) and source (z_s), although if $z_s \gg z_l$ this effect is minor. The lensing clusters are at redshifts between 0.19 and 0.41, and so the effect is small if $z_s \gtrsim 1$. A complete redshift distribution of SCUBA-selected galaxies is gradually being determined (Barger et al. 1998, 1999; Hughes et al. 1998; Lilly et al. 1998; Smail et al. 1998). Based on identifications made in high-quality optical images and extremely deep radio maps, and follow-up optical spectroscopy (Barger et al. 1999), we are able to distinguish which SCUBA galaxies are within the clusters, and in the foreground and background. The numbers of galaxies assigned to each category are listed in Table 1. It is likely that more than 80% of the *background* galaxies are at $z_s \lesssim 5$ (Smail et al. 1998), and no background candidates have been spectroscopically confirmed at $z_s < 0.9$ (Barger et al. 1999). Hence, $z_s \gtrsim 1$ for the background galaxies, and so is indeed expected to be much greater than z_l . Uncertainties in the redshift distribution of the SCUBA galaxies should not affect the derived counts significantly. The full sample of spectroscopic identifications of foreground/cluster/background galaxies span the redshift range 0.2 to 2.8; 14 out of the 17 detected galaxies have plausible identifications (Barger et al. 1999). The potential systematic errors due to these uncertainties are discussed in Section 3.1. At about the 15% level, they comprise a small contribution to the error budget in the count calculations.

3. MODELING THE COUNTS

Two approaches were taken to derive counts from our sub-mm maps and catalogs: a direct inversion of the

observed source catalog; and a Monte-Carlo method to constrain a parametric model for the background source counts. A comparison of the two techniques allows us to verify the reliability of the results.

3.1. Direct Inversion

The detailed mass models available for the seven clusters observed in the Smail et al. (1998) sample were used to reconstruct the counts of background galaxies by correcting for the effects of lensing. Due to the difficulties of incorporating incompleteness corrections in this method, we concentrated on the 80% ($> 4\sigma$) sample discussed by Smail et al. (1997, 1998). We also conducted the analysis using the more liberal 50% ($> 3\sigma$) sample, in order to both compare the results and assess the systematic error expected from the procedure. SCUBA detections identified with galaxies within the lensing clusters were excluded from our analysis. The number of galaxies identified with cluster sources and a foreground galaxy are listed in Table 1. At the faintest flux density, the 50% and 80% samples contain 8 and 14 non-cluster galaxies respectively.

Using the appropriate LENSTOOL models, the detected sources identified with background galaxies were mapped from their observed positions back onto the source planes at four values of $z_s = 1, 2, 3$ and 4. The flux densities of the galaxies were also corrected individually for lens amplification, leading to true flux densities in the source plane that are less than the observed values. Again we stress that this correction is only weakly dependent on redshift for our sources at $z_s \gtrsim 1$. None of the background SCUBA sources can be explained easily as multiple images of the same galaxy; however, such multiple images could be detected in deeper integrations. The number of galaxies in the catalog that are brighter than a flux density S , $N_{\text{raw}}(> S, z)$ is calculated at each redshift by simply counting the number of sources brighter than S in the source plane, after correcting for lensing. A simple Poisson uncertainty is attached to this value.

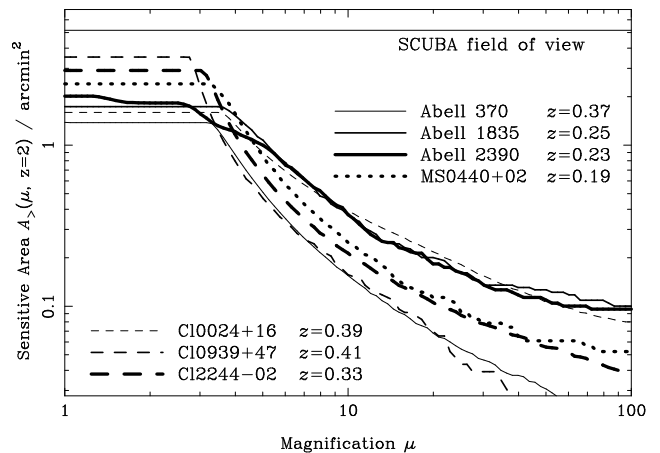


Fig. 1. The cumulative area of the source plane $A_>$, at $z_s = 2$, that experiences a magnification greater than μ for all seven clusters in the Smail et al. (1998) survey. The differences between clusters reflect their different redshifts and mass distributions. Low magnifications are absent because the SCUBA field of view encompasses only the concentrated cores of the clusters.

The area of background sky within which a galaxy would be detectable in each cluster was determined from a map of the magnification in the source plane, derived using the

LENSTOOL models. This quantity is also a weak function of redshift for $z_s \gtrsim 1$. The area of the source plane behind each cluster that lies within the SCUBA field of view, and is magnified by a factor greater than μ , $A_>$ is shown in Fig. 1, as an example for $z_s = 2$. Due to the magnification, $A_>$ is smaller than the SCUBA field of view.

A galaxy with a flux density S in the source plane will appear in the image plane of a particular cluster above a detection threshold S_{\min} if it is magnified by a factor greater than $\mu = S_{\min}/S$. The area in the source plane within which such a galaxy would be detected in that cluster is thus $A_>(S_{\min}/S, z)$. The flux density threshold S_{\min} and the form of $A_>$ are different for each cluster. By dividing the number of detected galaxies N_{raw} by the sum of the areas $A_>(S_{\min}/S, z)$ for all seven clusters, the cumulative count $N(> S, z) \simeq N_{\text{raw}}(> S, z) / \sum A_>(S_{\min}/S, z)$ is found. The count of identified foreground field galaxies is then calculated in the normal way and added to the result.

The count was calculated independently using this method for redshifts $z_s = 1, 2, 3$ and 4 . The spread in the results between these four cases as a function of flux density threshold is shown in Fig. 2. The results obtained from both the 50% and 80% samples at each redshift are compared with the mean count in each sample. The counts are remarkably consistent, reflecting partly that the value of the power-law index γ in the count $N(> S) \propto S^\gamma$ is $\gamma \lesssim -1$, indicating a small but positive magnification bias. The redshift-dependent scatter within the results obtained using both the 50% and 80% samples, is never more than 30%. Averaged over the range of flux densities from 0.5 to 8 mJy, the mean scatter is 12%. Providing that $z_s \gtrsim 1$ for background galaxies, as suggested by the initial spectroscopic results (Barger et al. 1999), the systematic uncertainty in the results due to the redshift distribution of the detected background galaxies is expected to be smaller than the absolute calibration uncertainties in the SCUBA images. These systematic uncertainties are included in the reported errors.

To reinforce this point, if the galaxies that are identified in the foreground of the clusters are assumed to be misidentified, and are actually background galaxies, then the counts at $S < 2$ mJy are expected to increase by about 0.5σ , with the brighter counts remaining the same. If all the background galaxies are assumed to be at $z_s = 4$, then the count at flux densities less than and greater than 2 mJy is expected to be reduced and increased by about 0.2σ respectively.

3.2. Parametric Simulations

To confirm the reliability of the results from the direct inversion we performed Monte-Carlo simulations of our observations using a parametric model for the background galaxy counts, and thus derived the best-fit parameters by comparison with the observations. This technique has the advantage that we can explicitly include the incompleteness of our maps at faint flux densities and so derive the counts separately for both the 80% and 50% samples. Galaxies were drawn from a population with a count described by a power-law model: $N(> S) = K(S/S_0)^\alpha$. For each realization we selected a value of K and α and populated the source planes of the seven clusters at random for each of the four values of redshifts used above. The source planes were then mapped onto the image planes using the

LENSTOOL models. The source catalogs derived from the areas of the images planes for each cluster covered by our SCUBA observations were then convolved with the appropriate incompleteness function determined by Smail et al. (1998), to determine the number of galaxies that would be detected in each cluster in the 50% and 80% samples. 1000 realizations of this process were executed for each set of model parameters $[K, \alpha]$ to derive a Monte-Carlo estimate of the count of background galaxies. As for the direct method, counts were calculated assuming $z_s = 1, 2, 3$ and 4 for the background galaxies. The predicted counts from each cluster and value of z_s were then added and compared with the observed counts for all seven clusters, assuming Poisson statistics, and the probability that the observed counts could be produced from each $[K, \alpha]$ pair was determined. The most probable values of K and α were determined at flux densities $S_0 = 1, 2$ and 4 mJy.

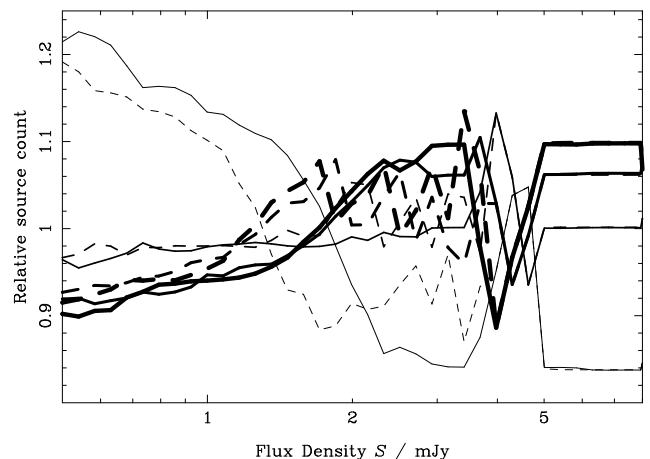


Fig. 2. The systematic differences in the inferred counts for the 80% Smail et al. (1998) sample (solid lines) for different assumed median redshifts for the sources. The line thickness increases in the order $z_s = 1, 2, 3$ and 4 . We also show the corresponding result for the 50% sample (dashed lines). The count values are normalized to the mean count derived from all four redshift values. There is little variation in the counts. At worst the counts for $z_s = 1$ and $z_s = 4$ differ by 30%. The mean scatter of the results about the mean for the four different redshifts between flux densities of 0.5 and 8 mJy is 12% in both the 50% and 80% samples. Note for comparison that the Poisson error on the counts is about 35%.

Table 1

The cumulative 850- μm counts deduced from both the direct analysis of the 80% sample and the Monte-Carlo analysis of both the 80% and 50% samples. Note that the errors on the counts are not independent, and that they should not be used to derive differential counts. The number of galaxies in the 80% and 50% samples that are brighter than each flux density, measured in the source plane, are given in the fifth and sixth columns, in the form of numbers of background/foreground/cluster galaxies.

Flux density / mJy	Direct count / 10^3 deg^{-2}	Monte-Carlo count K / 10^3 deg^{-2}	Monte-Carlo count slope α	$N_{80\%}$	$N_{50\%}$
0.5	22 ± 9	7/1/2	12/2/3
1.0	8.0 ± 3.0	8.6 ± 3.0	-1.3 ± 0.4	7/1/2	11/2/3
2.0	2.6 ± 1.0	3.9 ± 1.3	-1.4 ± 1.0	7/1/2	11/2/3
4.0	1.5 ± 0.7	1.4 ± 0.5	-1.8 ± 0.7	6/1/2	6/2/3
8.0	0.8 ± 0.6	3/1/1	3/1/1

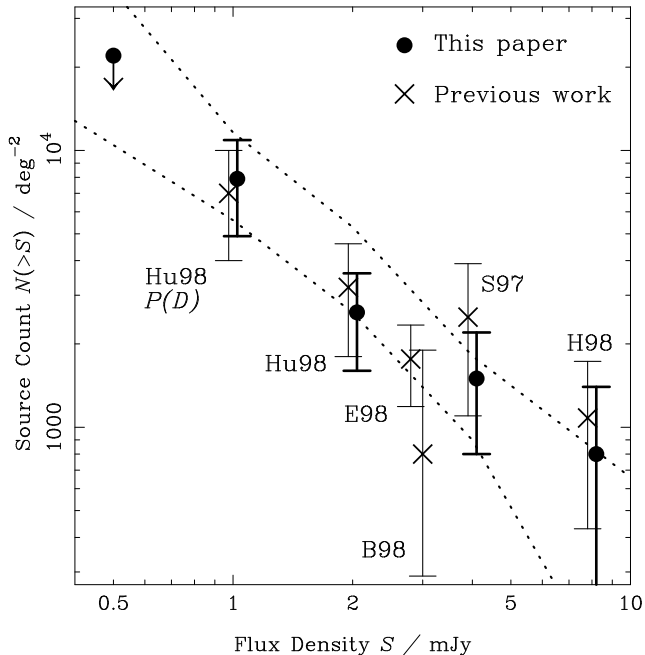


Fig. 3. Cumulative sub-mm counts corrected for lens magnification as listed in Table 1. The results obtained by direct inversion are shown by solid circles, while the $\pm 1\sigma$ bounds to the counts estimated from Monte-Carlo simulations are shown by dotted lines. Earlier counts from Barger et al. (1998; B98), Eales et al. (1998; E98), Holland et al. (1998; H98), Hughes et al. (1998; Hu98) and Smail et al. (1997; S97) are shown by crosses. $P(D)$ signifies the result of Hughes et al.'s confusion analysis.

4. RESULTS

The counts determined using both the direct and Monte-Carlo methods are listed in Table 1 and shown in Fig. 3. For both methods, the fractional errors obtained when the counts were calculated assuming redshifts $z_s = 1, 2, 3$ and 4 were very similar. The mean of these errors was used to define the final random error on the count. The quoted errors also include a systematic term, equal to the fractional spread of the results obtained for the 50% and 80% samples and for all four values of z_s . The errors reported in Table 1 are thus the most conservative that can be formulated from the data. In order to be maximally conservative, the faintest count at 0.5 mJy is plotted in Fig. 3, at the value listed in Table 1, but as an upper limit rather than a detection. It is possible for the counts to converge at a flux density just less than 1 mJy, but still remain consistent with the observed catalogs.

The direct and parametric estimates of the faint sub-mm counts in Table 1 and Fig. 3 are fully consistent, supporting the reliability and robustness of these results.

The new counts are deeper and more accurate than any

existing data, including the fluctuation analysis of the extremely deep SCUBA image of the *Hubble Deep Field* (Hughes et al. 1998). This shows the advantages of making sub-mm observations of cluster lenses for which accurate mass models are available. At brighter flux density levels, the results are coincident with and have comparable errors to the initial results of the SCUBA survey in Canada–France Redshift Survey fields (Eales et al. 1998).

By integrating over the counts brighter than 0.5 mJy, a 850- μm background radiation intensity of $(5 \pm 2) \times 10^{-10} \text{ W m}^{-2} \text{ sr}^{-1}$ in resolved sources is obtained. This is comparable to the current background radiation intensity obtained from *COBE* data by Fixsen et al. (1998).

5. CONCLUSIONS

By exploiting the magnification due to clusters of galaxies, we have determined the surface density of sub-mm-luminous galaxies down to a very faint flux density limit of 0.5 mJy at 850 μm , several times fainter than the confusion limit of the JCMT in blank fields. The results are consistent with those from an initial analysis of a subset of our catalog (Smail et al. 1997), and with the shallower counts from blank-field surveys. The errors on the counts are now reduced by a factor of two as compared with our earlier work. The count of 850- μm galaxies brighter than 1 mJy is $7900 \pm 3000 \text{ deg}^{-2}$. We have shown that the systematic errors due to both the uncertainties in the redshift distribution of the detected galaxies and the mass models of the clusters studied are less than 25%, and thus comparable to the absolute flux calibration of the SCUBA maps.

By summing the new counts down to their flux density limit, we have shown that our SCUBA maps resolve the major part of the 850- μm background radiation intensity into individual ultraluminous galaxies with luminosities greater than $10^{12} L_\odot$ (equivalent to star-formation rates greater than $100 M_\odot \text{ yr}^{-1}$ if no AGN contribution is present). Hence, most of the dust-enshrouded star-formation/AGN activity in the distant Universe took place in rare but extreme events.

Deeper SCUBA observations in the fields of rich lensing clusters will allow the counts ultimately to be pushed to even fainter flux densities than those achieved here, especially if an upgraded SCUBA becomes available. However, a significant improvement of our knowledge of the faint sub-mm-wave counts awaits the commissioning of a large mm-wave interferometer array.

ACKNOWLEDGEMENTS

We thank Malcolm Longair and an anonymous referee for helpful comments on the manuscript, the SCUBA com-

missioning team and Ian Robson for their help throughout the SCUBA lens survey, and the PPARC (RJI), Royal Society (IS) and MENRT (AWB) for support. This research

has been conducted under a European TMR network with generous support from the European Commission.

REFERENCES

- Barger, A. J., Cowie, L. L., Sanders, D. B., Fulton, E., Taniguchi, Y., Sato, Y., Kawara, K., & Okuda, H. 1998, *Nat*, 394, 248
- Barger, A. J., Cowie, L. L., Smail, I., Ivison, R. J., Blain, A. W., Kneib, J.-P., 1999, *AJ*, submitted
- Bézecourt, J., Kneib, J.-P., Soucaïl, G., & Ebbels, T., 1999, *A&A*, in press
- Blain, A. W. 1997, *MNRAS*, 290, 553
- Blain, A. W., Ivison, R. J., & Smail, I. 1998, *MNRAS*, 296, L29
- Blain, A. W., Smail, I., Ivison, R. J., & Kneib, J.-P. 1999, *MNRAS*, in press
- Eales, S. A., Lilly, S. J., Gear, W. K., Dunne, L., Bond, J. R., Hammer, F., Le Fèvre, O., & Crampton, D. 1998, *ApJ Letters*, submitted
- Edge, A. C., Smail, I., Ellis, R. S., Blandford, R. D., Ebeling, H., Allen, S. W., Fabian, A. C., & Kneib J.-P., 1999, in preparation
- Fixsen, D. J., Dwek, E., Mather, J. C., Bennett, C. L., & Shafer, R. A. 1998, *ApJ*, in press
- Gioia, I. M., Shaya, E. J., Le Fèvre, O., Falco, E. E., Luppino, G. A., & Hammer F. 1998, *ApJ*, 497, 573
- Holland, W. S. et al. 1999, *MNRAS*, in press
- Holland, W. S. et al. 1998, *Nat*, 392, 788
- Hughes, D. et al. 1998, *Nat*, 394, 241
- Ivison, R. J., Smail, I., Le Borgne, J.-F., Blain, A. W., Kneib, J.-P., Bézecourt, J., Kerr, T. H., Davies, J. K. 1998, *MNRAS*, 298, 583
- Kneib, J.-P., Mellier, Y., Fort, B., & Mathez, G. 1993, *A&A*, 273, 367
- Kneib, J.-P., Ellis, R. S., Smail, I., Couch, W. J., & Sharples, R. M. 1996, *ApJ*, 471, 643
- Kneib, J.-P. et al., 1999, in preparation
- Kneib, J.-P. 1998, private communication
- Lilly, S. J., Eales, S. A., Gear, W. K., Bond, J. R., Dunne, L., Hammer, F., Le Fèvre, O., & Crampton, D. 1998, in Benvenuti J. et al. eds., *NGST: Science Drivers and Technical Challenges*. ESA publications, Noordwijk, in press
- Seitz, C., Kneib, J.-P., Schneider, P., & Seitz, S. 1996, *A&A*, 314, 707
- Smail, I., Dressler, A., Kneib, J.-P., Ellis, R. S., Couch, W. J., Sharples, R. M., & Oemler, A. 1996, *ApJ*, 469, 508
- Smail, I., Ivison, R. J., & Blain, A. W. 1997, *ApJ*, 490, L5
- Smail, I., Ivison, R. J., Blain, A. W., & Kneib J.-P. 1998, *ApJ*, 507, L21
- Smail, I., et al. 1999, in preparation